

Time-aware Metapath Feature Augmentation for Ponzi Detection in Ethereum

Chengxiang Jin, Jiajun Zhou, Jie Jin, Jiajing Wu, *Senior Member, IEEE*, Qi Xuan, *Senior Member, IEEE*

Abstract—With the development of Web 3.0 which emphasizes decentralization, blockchain technology ushers in its revolution and also brings numerous challenges, particularly in the field of cryptocurrency. Recently, a large number of criminal behaviors continuously emerge on blockchain, such as Ponzi schemes and phishing scams, which severely endanger decentralized finance. Existing graph-based abnormal behavior detection methods on blockchain usually focus on constructing homogeneous transaction graphs without distinguishing the heterogeneity of nodes and edges, resulting in partial loss of transaction pattern information. Although existing heterogeneous modeling methods can depict richer information through metapaths, the extracted metapaths generally neglect temporal dependencies between entities and do not reflect real behavior. In this paper, we introduce Time-aware Metapath Feature Augmentation (*TMFAug*) as a plug-and-play module to capture the real metapath-based transaction patterns during Ponzi scheme detection on Ethereum. The proposed module can be adaptively combined with existing graph-based Ponzi detection methods. Extensive experimental results show that our *TMFAug* can help existing Ponzi detection methods achieve significant performance improvements on the Ethereum dataset, indicating the effectiveness of heterogeneous temporal information for Ponzi scheme detection.

Index Terms—Ponzi scheme detection; Metapath; Temporal information; Heterogeneous graph; Ethereum; Blockchain.

I. INTRODUCTION

BLOCKCHAIN technology has been developing rapidly in recent years and gradually gaining public attention. Blockchain [1] is a peer-to-peer network system based on technologies such as cryptography [2] and consensus mechanisms [3] to create and store huge transaction information. At present, the biggest application scenario of blockchain technology is cryptocurrency. For example, the initial “Bitcoin” [4] also represents the birth of blockchain. As cryptocurrencies

continue to evolve, smart contracts [5] bring blockchain 2.0, also known as Ethereum [6]. Unlike Bitcoin, which prefers a peer-to-peer electronic cash system, Ethereum is a platform for decentralized applications and allows anyone to create and execute smart contracts. The smart contract [7], accompanying Ethereum, is understood as a program on the blockchain that operates when the starting conditions are met. Since smart contracts operate on publicly accessible code and are immutable, it is possible to carry out secure transactions without third-party endorsement.

The Ponzi scheme [8] is a form of fraud that benefits from a poor return on investment to the victim. Traditional Ponzi schemes have existed only offline, but they have gradually taken on an online form as the spotlight of money flows has shifted online. Cryptocurrency is trusted by the public for its security. Due to the transparency and immutability of smart contracts on Ethereum, people tend to be less vigilant, which makes it easier for Ponzi schemes to execute. According to recent reports¹, the SEC revealed that the Forsage smart contract platform [9] is a large fraudulent pyramid scheme that marketed fraudulent products to investors, involving a total of \$300 million and millions of victims. This undermines the public’s trust in cryptocurrencies. Therefore, there is an urgent need to understand the behavior of Ponzi schemes and detect them from cryptocurrency platforms, further maintaining the stability of the investment environment in financial markets.

Existing Ponzi scheme detection methods based on graph analytics generally rely on homogeneous graph modeling [10], [11] due to their simplicity. However, real transactions on Ethereum generally involve different types of interactions between different types of accounts, which will be neglected during homogeneous modeling. Therefore, it is tough to reflect the complexity and diversity in real transactions simply by homogeneous graphs. Meanwhile, heterogeneous graph [12] is a widely used technique to model complex interactions, which can preserve the semantic information of interactions to the greatest extent. Typical heterogeneous techniques generally employ the metapath structure [13] to capture the specific interaction patterns. However, several approaches [14], [15] are obsessed with searching for the best metapaths, which is time-consuming and difficult to define the best. In addition, the timestamp information will be neglected when extracting metapaths, resulting in an inappropriate afterthought. Finally, compared with homogeneous methods, heterogeneous meth-

This work was partially supported by the National Key R&D Program of China under Grant 2020YFB1006104, by the Key R&D Programs of Zhejiang under Grants 2022C01018 and 2021C01117, by the National Natural Science Foundation of China under Grant 61973273, and by the Zhejiang Provincial Natural Science Foundation of China under Grant LR19F030001.

C. Jin, J. Zhou, J. Jin are with the Institute of Cyberspace Security, College of Information Engineering, Zhejiang University of Technology, Hangzhou 310023, China. E-mail: {2112103081, jjzhou, 2112003197}@zjut.edu.cn.

J. Wu is with the School of Computer Science and Engineering, Sun Yat-sen University, Guangzhou 510006, China. E-mail: wujiajing@mail.sysu.edu.cn.

Q. Xuan is with the Institute of Cyberspace Security, College of Information Engineering, Zhejiang University of Technology, Hangzhou 310023, China, with the PCL Research Center of Networks and Communications, Peng Cheng Laboratory, Shenzhen 518000, China, and also with the Utron Technology Co., Ltd. (as Hangzhou Qianjiang Distinguished Expert), Hangzhou 310056, China. E-mail: xuanqi@zjut.edu.cn.

C. Jin and J. Zhou make equal contribution.

Corresponding author: Jiajun Zhou.

¹<https://www.sec.gov/news/press-release/2022-134>

ods ensure fine granularity of information, but also bring operational complexity.

The aforementioned issues motivate us to improve Ponzi detection by integrating heterogeneous information and time information into homogeneous methods. In this paper, we propose Time-aware Metapath Feature Augmentation (*TMFAug*) as a generic module to capture the temporal behavior patterns hidden in Ethereum interaction graph. Specifically, *TMFAug* first extracts the time-aware metapath features on an auxiliary heterogeneous graph where the coordinated transaction and contract call information are contained, and then aggregates these heterogeneous features associated with temporal behavior patterns to corresponding account nodes in the homogeneous graph where the Ponzi detection methods are performed. Our proposed module allows for improving the performance of existing Ponzi detection methods through feature augmentation without adjusting them.

The main contributions of this work are summarized as follows:

- We collect labeled ethereum Ponzi scheme data for Ponzi detection research.
- We propose a generic time-aware metapath feature augmentation module, named *TMFAug*, which allows for aggregating heterogeneous features associated with temporal behavior patterns to homogeneous transaction graphs, further improving the performance of existing Ponzi detection methods. To the best of our knowledge, there are hardly any heterogeneous algorithms applied to blockchain data mining, and our work earlier explored the heterogeneous strategies for Ethereum Ponzi detection.
- Extensive experiments on the Ethereum dataset demonstrate that the *TMFAug* module can effectively improve the performance of multiple existing Ponzi detection methods. Moreover, the generic compatibility of *TMFAug* also suggests that temporal and heterogeneous behavior pattern information can benefit Ponzi scheme detection in Ethereum.

The remaining portions of this paper are summarized below. Sec. II reviews the related work in graph representation learning and graph-based Ponzi detection methods. Sec. III describes the details of constructing an account interaction graph on Ethereum. Sec. IV introduces the details of the proposed *TMFAug* module. The experimental settings and analysis are presented in Sec. V. Finally, we conclude this paper and prospect future work in Sec. VI.

II. RELATED WORK

In this section, we review several established graph-related methods and introduce their applications in Ethereum Ponzi scheme detection.

A. Graph Representation Learning

Graph representation learning aims to generate low-dimensional vectors that capture the properties and structure of graphs. Early related works focus on learning topological embeddings, classical ones include Deepwalk, Line, and Node2Vec. Deepwalk [16] first generates node sequences by

TABLE I
NOTATIONS AND DESCRIPTIONS.

Notation	Description
G_{hom}	Homogeneous graph
G_{het}	Heterogeneous graph
\mathbf{x}	Account feature
$\hat{\mathbf{x}}$	Account feature with <i>TMFAug</i>
\mathcal{P}	Time-aware Metapath
\mathcal{P}	Super metapath
\mathcal{P}_i	The i -th category of super metapath
$\vec{\mathcal{V}}(\mathcal{P})$	The node sequence of the super metapath
\mathcal{M}	The set of super metapath with same head node
\mathcal{M}_*	The set of super metapath with same target node
ω	The important attribute of the super metapath
$\hat{\omega}$	The normalized attribute of the super metapath

random walks, then regards them as sentences and feeds into language model for learning node representations. On this basis, Node2Vec [17] introduces two parameters to control the trade-off between the breadth-first search and depth-first search of random walks in order to better capture the topological characteristics. Line [18] is applicable to various kinds of networks as well as large networks and takes into account the first-order and second-order similarities between nodes. The above methods are task-agnostic and only focus on the topology of the graph, which generally leads to mediocre performance on downstream tasks. Graph neural networks (GNNs) simultaneously learn the attribute features and topological features of graphs, which brings graph representation learning to a new level. As a pioneer in GNNs, GCN [19] is a semi-supervised learning method that first applies the convolutional algorithm in the graph. Following GCN, GAT [20] considers the importance of neighbors and introduces self-attention mechanism to assign an aggregated weight to each neighbor. On the other hand, GraphSAGE [21] uses the sampling strategy to transform the full graph training into subgraph mini-batch training, which greatly improves the scalability of GNN on large graph computation. Additionally, GIN [22] defines the graph neural network expressivity problem and designs an injective neighbor aggregation function in a simple setup formalism.

B. Graph-based Ponzi Schemes Detection in Ethereum

In 1919, a speculative businessman named Charles Ponzi made fictitious investments in a company with the intention of luring other individuals into the scam by promising new investors a quick return on their initial investment. Consequently, this type of fraud is known as a Ponzi scheme. Traditional Ponzi schemes were offline, while recently there has been a shift to online. Moore et al. [23] described a type of high-yield investment program (HYIPs), an online Ponzi scheme. They argued that some investors know well the fraudulent nature of these sites, but they believe they can gain partial benefit by investing early in the Ponzi and withdrawing their funds before the Ponzi scheme collapses. This idea makes it

easy for Ponzi fraudsters to obtain the initial investment. As time goes by, HYIPs are also active in cryptocurrencies. Vasek et al. [24] analyzed the behavior of Ponzi schemes involving Bitcoin in HYIPs, which they called Bitcoin-only HYIPs. They introduced a variety of fraudulent methods, such as one part claiming to be a legitimate investment vehicle, another part claiming to be an online bitcoin wallet that offers high daily returns, etc.

Analysis of HYIPs has revealed that a number of traditional Ponzi schemes have gradually emerged in cryptocurrencies, generating unique means of deception. For example, due to the non-interruptible nature of smart contracts, a lack of attention to contract content can lead to the failure to withdraw funds before a Ponzi scheme collapses, thus amplifying the losses of less sophisticated investors. Nowadays, multiple detection methods have been proposed to mitigate the damage caused by Ponzi schemes.

Many existing Ponzi scheme detection methods are performed on complex transaction networks. Chen et al. [25] constructed transaction and code features, and feed them into downstream machine learning classifier to identify Ponzi schemes. Since feature engineering is hard to depict more complex transaction behavior, Chen et al. [26] utilized graph embedding to automatically learn high-expressive code features. In order to improve a combination of feature engineering and machine learning, Fan et al. [27] trained a Ponzi scheme detection model using the idea of ordered augmentation. Zhang et al. [28] proposed a new method for Ethereum Ponzi scheme detection based on an improved LightGBM algorithm with Smote + Tomek, which can alleviate the imbalance problem of Ponzi data. Yu et al. [29] constructed transaction graphs and utilized GCN [19] to characterize the account features for Ponzi detection. Zhang et al. [30] constructed multi-granularity data in opcodes and proposed a novel multi-granularity multi-scale convolutional neural network model for Ponzi scheme detection. Timestamp information is very important for modeling temporal transaction behavior. Bartoletti et al. [31] investigated the role of temporal behavior in Ponzi detection and developed time-dependent features. Jin et al. [32] used both transaction information and code information to propose a dual-view Ponzi scheme early warning framework, while introducing a temporal evolution augmentation strategy to augment the limited Ponzi dataset.

However, the above-mentioned Ponzi detection methods suffer from several shortcomings. The above methods rely on homogeneous graphs, and neglect timestamps information and the types of nodes and edges, which makes it difficult to capture more complex and temporal behavior patterns. Jin et al. [33] explored this problem on Ethereum Ponzi detection, and proposed to fuse heterogeneous information in metapaths and their subsets, further enhancing existing Ponzi detection methods. However, they neglected the timestamp information so that the constructed metapaths can not reflect the real behavior patterns. Therefore, in this paper, we focus more on capturing certain temporal and structural information from metapaths, and work on the integration of heterogeneous and temporal information into homogeneous approaches for Ponzi scheme detection.

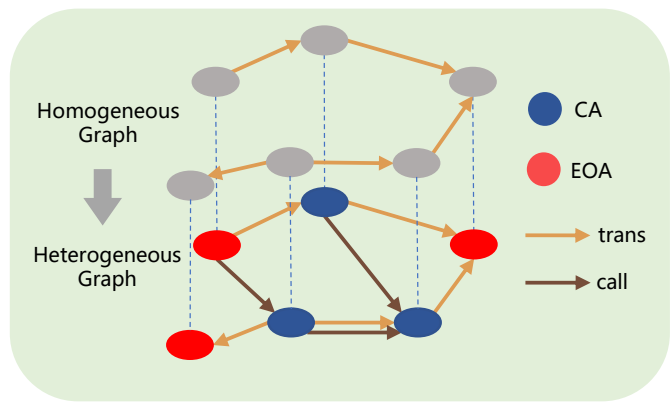


Fig. 1. Homogeneous transaction graph and heterogeneous interaction graph.

III. ACCOUNT INTERACTION GRAPH MODELING

In this section, we focus on modeling Ethereum transaction data as account interaction graphs, as well as providing a brief introduction to Ethereum data.

A. Ethereum Data

An account in Ethereum is an entity that owns Ether and can be divided into two categories: Externally Owned Account (EOA) and Contract Account (CA) [6]. EOA is controlled by a user with a private key and can initiate transactions on Ethereum, and CA is controlled by smart contract code and can only get triggers to implement the contract function. There are generally two categories of interactions between Ethereum accounts: transaction and contract call. The transaction is the process by which an action is initiated by an EOA and received by another EOA, or ultimately back to itself. Contract calls, which are divided into external calls and internal calls, refer to the process of triggering a smart contract code that can execute many different actions, such as transferring tokens or creating a new contract.

B. Graph Modeling on Ethereum

The existing Ponzi scheme detection methods mainly use homogeneous transaction graphs, which regard all nodes and edges as the same type, neglecting the complex and temporal interaction information. On the contrary, heterogeneous graphs group nodes and edges into various categories, which can represent more complex interaction scenarios and make full use of graph information. Considering that most of the existing Ponzi detection methods are only suitable for homogeneous graphs, we consider extracting information from heterogeneous graphs to assist in Ponzi detection on homogeneous graphs.

More formally, we use $G_{hom} = (V, E, Y)$ and $G_{het} = (V_{eoa}, V_{ca}, E_{trans}^t, E_{call}^t, Y)$ to represent the two types of graphs respectively, where V represents the set of accounts in the Ethereum data, V_{eoa} and V_{ca} represent the sets of EOA and CA respectively, E represents the set of directed edges constructed from transaction information, E_{trans}^t and E_{call}^t represent the sets of directed edges with timestamps constructed from transaction information and contract call information respectively,

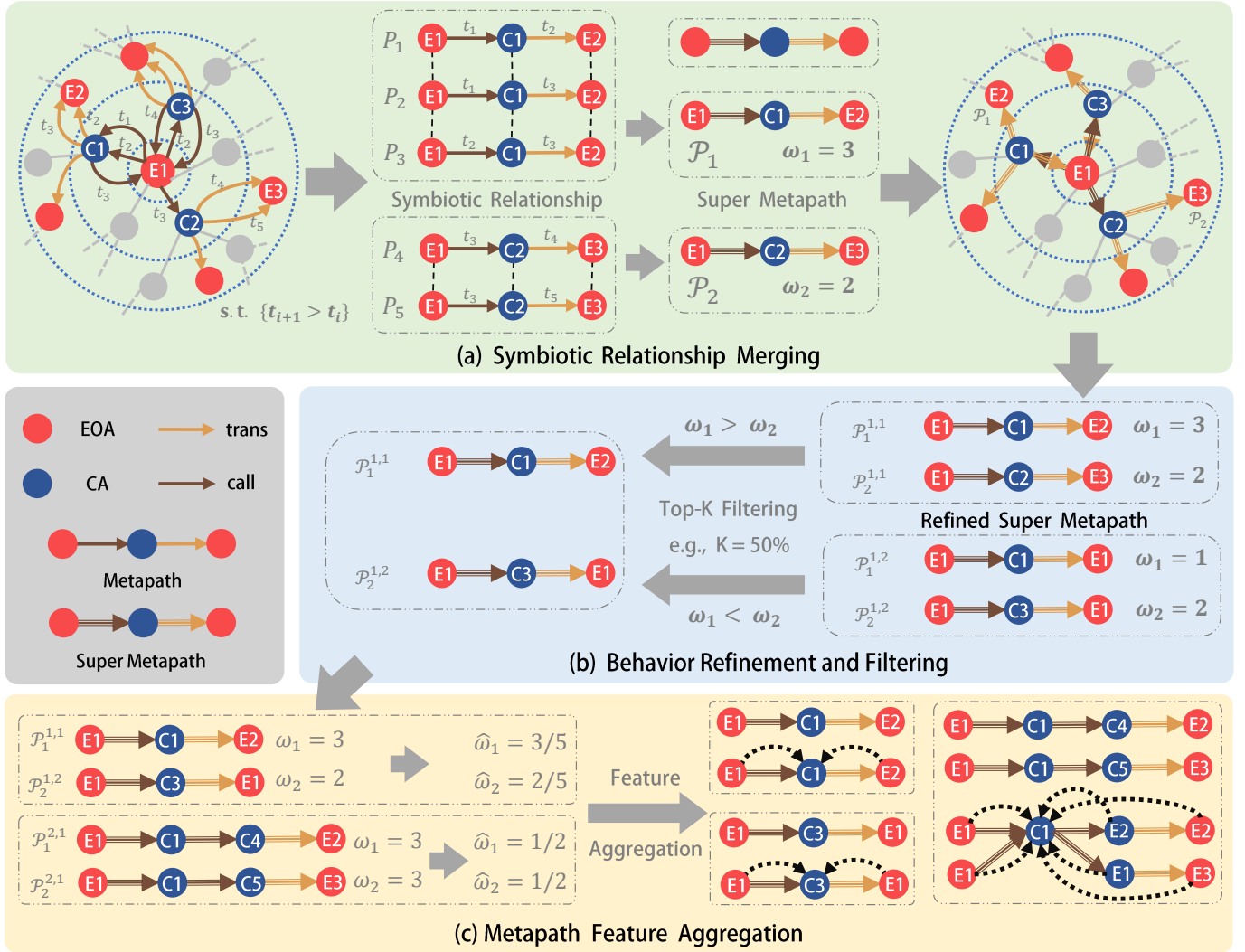


Fig. 3. The overall framework of the Time-aware Metapath Feature Augmentation. The complete workflow proceeds as follows: (a) merging symbiotic relations to obtain the super metapaths; (b) refining the super metapaths based on the behavior, and filtering the super metapaths by Top- K ; (c) aggregating the information along metapaths to the target nodes.

Ponzi schemes reward old investors through new investment income, i.e., two-way transactions do not occur simultaneously, so here we introduce the time information of transactions to depict the temporal behavior patterns. Formally, we use the following **time-aware metapath** to characterize the temporal behavior patterns:

$$EOA_1 \xrightarrow{t_1} CA_* \left(\xrightarrow{t_2} CA_1 \right) \xrightarrow{t_3} EOA_2 \quad (3)$$

s.t. $t_1 < t_2 < t_3$

Note that the timing constraint $t_1 < t_2 < t_3$ ensures that the behavior pattern represented by the metapath is more consistent with the real interaction law. Additionally, we call the metapath defined in Eq. (2) a timeless metapath, which ignores the timing of interactions and is based on an after-the-fact perspective.

Furthermore, the temporal behavior patterns defined in

Eq. (3) can be divided into two cases:

$$\begin{aligned} P^1 &: EOA \xrightarrow[t_1]{call} CA_* \xrightarrow[t_2]{trans} EOA \\ P^2 &: EOA \xrightarrow[t_1]{call} CA_* \xrightarrow[t_2]{call} CA \xrightarrow[t_3]{trans} EOA \end{aligned} \quad (4)$$

We use P^1 and P^2 to represent the two types of temporal behavior patterns which have been described above.

B. Symbiotic Relationship Merging

There are usually frequent interactions between multiple accounts, yielding multiple metapaths with the same sequences of nodes and relationships, but different sequences of timestamps. Here we consider these metapaths to be symbiotic with each other and introduce the definition of a symbiotic relationship as follows:

Definition 1: Symbiotic Relationship. For a pair of time-aware metapaths (P_1, P_2) , they are symbiotic if and only if

they have the same node sequence and relation sequence, i.e.,

$$\begin{aligned} P_1 &\cong P_2 \\ \text{s.t. } \vec{V}(P_1) &= \vec{V}(P_2), \quad \vec{R}(P_1) = \vec{R}(P_2) \end{aligned} \quad (5)$$

where \cong represents a symbiotic relationship, \vec{V} and \vec{R} represent the node sequence and relationship sequence, respectively.

As illustrated in Fig. 3(a), P_1 , P_2 and P_3 are symbiotic to each other because they have the same sequences of nodes and relationships $E1 \xrightarrow{\text{call}} C1 \xrightarrow{\text{trans}} E2$, and so do P_4 and P_5 . Since symbiotic metapaths are numerous and have the same form, we use a super metapath to substitute them. Specifically, given a set of symbiotic metapaths $\{P_1, P_2, \dots, P_n \mid P_1 \cong P_2 \cong \dots \cong P_n\}$, we merge these symbiotic metapaths into a super metapath \mathcal{P} . Intuitively, the number of symbiotic metapaths reflects the account's preference in participating in this behavior to a certain extent. So we measure the importance of the super metapath via the number of symbiotic metapaths and further assign it an importance attribute $\omega = n$. As illustrated in Fig. 3(a), $\{P_1, P_2, P_3\}$ (or $\{P_4, P_5\}$) is merged into a super metapath \mathcal{P}_1 (or \mathcal{P}_2) and assigned an importance attribute $\omega_1 = 3$ (or $\omega_2 = 2$).

C. Behavior Refinement and Filtering

The temporal behavior patterns defined in Eq. (4) are coarse-grained, and we can further refine them into six cases according to the different behavior patterns of Ponzi accounts and normal accounts.

- $P^{1,1} : EOA_1 \xrightarrow[t_1]{\text{call}} CA_* \xrightarrow[t_2]{\text{trans}} EOA_2$

It reflects four behavior patterns: 1) ponzi account accepts new external investment and then rewards old investor; 2) ponzi account accepts new external investment and then transfers commission to the fraudster; 3) fraudster invests and rewards himself to attract external investors; 4) fraudster sweeps commission.

- $P^{1,2} : EOA_1 \xrightarrow[t_1]{\text{call}} CA_* \xrightarrow[t_2]{\text{trans}} EOA_1$

It reflects three behavior patterns: 1) ponzi account accepts new external investment and rewards this investor later; 2) fraudster invests and rewards himself to attract external investors; 3) fraudster sweeps commission.

- $P^{2,1} : EOA_1 \xrightarrow[t_1]{\text{call}} CA_* \xrightarrow[t_2]{\text{call}} CA_2 \xrightarrow[t_3]{\text{trans}} EOA_2$

This metapath reflects four behavior patterns, which are similar to $P^{1,1}$.

- $P^{2,2} : EOA_1 \xrightarrow[t_1]{\text{call}} CA_* \xrightarrow[t_2]{\text{call}} CA_2 \xrightarrow[t_3]{\text{trans}} EOA_1$

This metapath reflects three behavior patterns, which are similar to $P^{1,2}$.

- $P^{2,3} : EOA_1 \xrightarrow[t_1]{\text{call}} CA_* \xrightarrow[t_2]{\text{call}} CA_* \xrightarrow[t_3]{\text{trans}} EOA_2$

$P^{2,4} : EOA_1 \xrightarrow[t_1]{\text{call}} CA_* \xrightarrow[t_2]{\text{call}} CA_* \xrightarrow[t_3]{\text{trans}} EOA_1$

After analyzing the extracted metapaths, we find that the behavior patterns involving contract self-call only occur in normal interactions.

According to the heterogeneous interaction graph constructed in Table II, we count the number of all coarse and refined metapaths, as reported in Table III. It is clear that there are significant quantitative differences between different

TABLE III
STATISTICS OF TIME-AWARE METAPATHS.

Metapath	$P^{1,1}$	$P^{1,2}$	$P^{2,1}$	$P^{2,2}$	$P^{2,3}$	$P^{2,4}$	Sum
P^1	3,275,459,278	4,851,608	-	-	-	-	3,280,310,886
P^2	-	-	37,895	2,671	9,229	254	50,049

types of metapaths. After getting all the refined symbiotic metapaths and merging them into refined super metapaths, we perform Top- K filtering to preserve the most important metapaths. The Top- K filtering is guided by the importance attribute ω of the super metapaths, following the intuition that frequent behavior patterns are more favorable for account feature characterization. As illustrated in Fig. 3(b), for each kind of refined super metapaths $\mathcal{P}^{1,1}$ (or $\mathcal{P}^{1,2}$), those with larger attribute values will be preserved, such as $\mathcal{P}_1^{1,1}$ (or $\mathcal{P}_2^{1,2}$).

D. Metapath Feature Aggregation

The above two steps aim to obtain the important behavior information represented by super metapaths, and the super metapaths retained during Top- K filtering will participate in the subsequent feature aggregation step. *TMFAug* is designed to fuse the behavior features represented by metapaths and finally enhance existing Ponzi detection methods on homogeneous Ethereum interaction graph. However, the preserved super metapaths are still numerous. In order to alleviate information redundancy and feature explosion during metapath feature aggregation, we adjust the importance attribute of super metapaths before doing so. Specifically, for super metapaths starting from the same head node v_{eoa} , we first group them as follows:

$$\mathcal{M}^\square = \{\mathcal{P}_i^\square \mid \vec{V}(\mathcal{P}_i^\square)[1] = v_{eoa}\}, \quad \text{s.t. } \square \in \{1, 2\} \quad (6)$$

where $\vec{V}(\mathcal{P})[1]$ represents getting the first element in the node sequence (i.e., head node) of super metapath \mathcal{P} . Then we compute the normalized importance attribute for each super metapath \mathcal{P}_i^\square in \mathcal{M}^\square as follows:

$$\hat{\omega}_i^\square = \omega_i^\square / \sum_{\mathcal{P} \in \mathcal{M}^\square} \omega, \quad \text{s.t. } \square \in \{1, 2\} \quad (7)$$

After adjusting the importance attribute of all the super metapaths, we then perform feature aggregation to update the CA features. Specifically, for a target CA node v_{ca}^* (CA_* in Eq. (3)), we first group the super metapaths that contain it as follows:

$$\mathcal{M}_*^\square = \{\mathcal{P}_i^\square \mid \vec{V}(\mathcal{P}_i^\square)[2] = v_{ca}^*\}, \quad \text{s.t. } \square \in \{1, 2\} \quad (8)$$

After grouping the super metapaths, we update the features of the target CA by aggregating the features of other nodes in the metapath, and the final target CA feature is obtained by processing multiple super metapaths of the same group, as illustrated in Fig. 3(c). The process of feature update can be represented as follows:

$$\hat{x}_{ca}^\square = \sum_{\mathcal{P} \in \mathcal{M}_*^\square} \hat{\omega} \cdot \sum_{v \in \vec{V}(\mathcal{P})} \mathbf{x}_v, \quad \text{s.t. } \square \in \{1, 2\} \quad (9)$$

TABLE IV

PONZI DETECTION RESULTS OF RAW METHODS AND THEIR ENHANCED VERSIONS (WITH *TMFAug* OR *MFAug*) IN TERMS OF MICRO-F1 (GAIN), AND GAIN REPRESENTS THE RELATIVE IMPROVEMENT RATE. THE ENHANCED RESULTS ARE MARKED WITH BOLDFACE. AVG. RANK REPRESENTS THE AVERAGE RANK.

Method	Manual Feature		Line		DeepWalk		Node2Vec		GNN				Avg. Rank
	SVM	RF	SVM	RF	SVM	RF	SVM	RF	GCN	GAT	GIN	SAGE	
raw	73.03	73.32	76.98	76.97	83.00	81.43	84.56	86.13	84.50	84.24	84.59	85.70	6.33
<i>MFAug</i> (\mathcal{P}^1)	71.20 (-2.51%)	76.45 (+4.27%)	76.19 (-1.03%)	77.49 (+6.68%)	85.09 (+2.52%)	83.79 (+2.90%)	86.15 (+1.87%)	86.40 (+0.31%)	85.71 (+1.43%)	87.06 (+3.35%)	85.33 (+0.87%)	86.75 (+1.23%)	3.83
<i>TMFAug</i> (\mathcal{P}^1)	71.98 (-1.44%)	75.65 (+3.18%)	76.98 (+0.00%)	76.18 (-1.03%)	85.09 (+2.52%)	84.31 (+3.54%)	86.15 (+1.87%)	86.92 (+0.92%)	85.71 (+1.43%)	87.59 (+3.98%)	85.08 (+0.58%)	86.91 (+1.41%)	3.50
<i>MFAug</i> (\mathcal{P}^2)	73.30 (+0.37%)	76.44 (+3.26%)	78.02 (+1.35%)	78.27 (+1.69%)	85.09 (+2.52%)	83.00 (+1.93%)	85.08 (+0.61%)	87.19 (+1.23%)	85.71 (+1.43%)	86.60 (+2.89%)	85.86 (+1.59%)	86.65 (+1.11%)	3.33
<i>TMFAug</i> (\mathcal{P}^2)	73.83 (+1.11%)	75.93 (+3.56%)	78.28 (+1.69%)	79.33 (+3.07%)	84.82 (+2.19%)	84.57 (+3.36%)	85.36 (+0.95%)	86.41 (+0.33%)	86.39 (+2.24%)	87.12 (+3.42%)	86.38 (+2.12%)	86.86 (+1.35%)	2.75
<i>MFAug</i> ($\mathcal{P}^1 + \mathcal{P}^2$)	73.03 (+0.00%)	76.97 (+4.98%)	75.40 (-2.05%)	76.19 (-1.01%)	85.09 (+2.52%)	84.83 (+1.18%)	86.67 (+2.50%)	86.66 (+0.62%)	85.60 (+1.30%)	87.06 (+3.35%)	86.12 (+1.81%)	86.06 (+0.42%)	3.42
<i>TMFAug</i> ($\mathcal{P}^1 + \mathcal{P}^2$)	72.25 (-1.07%)	76.96 (+4.96%)	76.98 (+0.00%)	77.23 (+0.32%)	85.09 (+2.52%)	83.26 (+2.25%)	86.15 (+1.87%)	86.66 (+0.62%)	85.92 (+1.68%)	87.68 (+4.08%)	85.08 (+0.58%)	86.59 (+0.04%)	3.17

where x_v is the initial account feature of nodes along the metapath. Finally, the updated features \hat{x} contain heterogeneous structural information associated with temporal behavior patterns and will be fed into the downstream classification task.

V. EXPERIMENT

In this section, we evaluate the effectiveness of our *TMFAug* on improving Ponzi scheme detection by answering the following research questions:

- **RQ1:** Can our *TMFAug* improve the performance of Ponzi scheme detection when combined with existing detection methods?
- **RQ2:** Whether time information can help capture more effective behavior patterns?
- **RQ3:** How do different behavior patterns affect the detection results?
- **RQ4:** How does the behavior refinement affect the detection results?
- **RQ5:** How does the behavior filtering affect the detection results?

A. Data

We crawled 191 labeled Ponzi data from *Xblock*¹, *Etherscan*² and other Blockchain platforms. For all detection methods, we take all the labeled Ponzi accounts as positive samples, as well as the same number of randomly sampled CA as negative samples. The construction details of the homogeneous transaction graph and the heterogeneous interaction graph are described in Sec. III-B and Table II.

B. Ponzi Detection Methods and Experimental Setup

To illustrate the effectiveness of our *TMFAug* module, we combine it with three categories of Ponzi detection methods: manual feature engineering, graph embedding and GNN-based methods. And we also introduce a *MFAug* module for comparison, which uses timeless metapaths for feature augmentation.

Manual feature engineering is the most common and simplest approach for Ponzi detection, we use 15 manual features listed in Sec. III-C to construct the initial features for account nodes. For Ponzi detection based on graph embedding, we

consider DeepWalk, Node2Vec and Line algorithms for constructing the initial account node features, respectively. For the above two categories of methods, we achieve Ponzi detection by feeding the generated account features into two machine learning classifiers: Support Vector Machine (SVM) [34] and Random Forest (RF) [35]. When combined with *TMFAug*, we feed the updated features generated via *TMFAug* into the downstream classifiers. For GNN-based methods, we use four popular GNNs: GCN, GAT, GIN and GraphSAGE, with the same initial features as manual feature engineering.

For DeepWalk and Node2Vec, we set the dimension of embedding, window size, walk length and the number of walks per node to 128, 10, 50 and 5 respectively. For Node2Vec, we perform a grid search of return parameter p and in-out parameter q in $\{0.5, 1, 2\}$. For Line, we set the embedding dimension and order to 32 and 2, respectively. For GNN-based methods, we set the hidden dimension of GCN, GAT, GIN and GraphSAGE to 128, 32, 128 and 128 respectively, and the learning rate to 0.01, 0.1, 0.1 and 0.01 respectively. For filtering parameter K , we vary in $\{1\%, 3\%, 5\%, 7\%, 9\%, 10\%, 20\%, 30\%, 40\%, 50\%\}$ and choose the best results for Ponzi detection. For all methods, we repeat 5-fold cross-validation five times and report the average micro-F1 score.

C. Enhancement for Ponzi Detection (RQ1)

Table IV report the results of performance comparison between the raw methods and their enhanced version (with *TMFAug*), from which we can observe that there is a significant boost in detection performance across all methods. Overall, these detection methods combined with *TMFAug* module obtain higher average detection performance in most cases, and the *TMFAug* achieves a 86.11% success rate¹ on improving Ponzi detection. Specifically, with the exception of partial results of manual feature engineering and Line, our *TMFAug* achieves consistent performance enhancement, yielding 1.11% ~ 4.96%, 0.32% ~ 3.86%, 0.58% ~ 4.58% relative improvement on the three categories of detection methods, respectively. It's worth noting that detection methods with higher initial performance are generally more likely to receive positive gains from our *TMFAug*. In this regard, we

¹<http://xblock.pro/ethereum/>

²<https://cn.etherscan.com/accounts/label/ponzi>

¹The success rate refers to the percentage of enhanced methods with F1 score higher than that of the corresponding raw methods.

TABLE V

ABLATION STUDY ON BEHAVIOR REFINEMENT AND FILTERING. (W/O REFINEMENT) REPRESENTS THE *TMFAug* WITHOUT BEHAVIOR REFINEMENT, AND (W/O FILTERING) REPRESENTS THE *TMFAug* WITHOUT BEHAVIOR FILTERING. THE BOLD MARKER REPRESENTS THE BETTER RESULT BETWEEN *TMFAug* WITH AND WITHOUT BEHAVIOR REFINEMENT, AND THE UNDERLINE REPRESENTS THE BETTER RESULT BETWEEN *TMFAug* WITH AND WITHOUT BEHAVIOR FILTERING. AVG.LOCAL RANK REPRESENTS THE AVERAGE RANK WITH DIFFERENT SUPER METAPATH.

Method	Manual Feature		Line		DeepWalk		Node2Vec		GNN				Avg. Local Rank
	SVM	RF	SVM	RF	SVM	RF	SVM	RF	GCN	GAT	GIN	SAGE	
<i>TMFAug</i> (\mathcal{P}^1) (w/o refinement)	72.26	76.19	76.98	75.91	85.09	84.05	86.14	87.18	85.76	87.32	85.34	86.62	1.67
<i>TMFAug</i> (\mathcal{P}^1) (w/o filtering)	67.28	70.17	58.13	68.63	82.47	<u>84.57</u>	86.13	85.88	<u>86.43</u>	83.25	<u>86.64</u>	84.97	2.50
<i>TMFAug</i> (\mathcal{P}^1)	<u>71.98</u>	<u>75.65</u>	<u>76.98</u>	76.18	<u>85.09</u>	84.31	86.15	<u>86.92</u>	85.71	87.59	85.08	86.91	1.67
<i>TMFAug</i> (\mathcal{P}^2) (w/o refinement)	73.82	75.67	77.76	79.32	85.09	83.79	85.36	86.93	86.18	87.22	85.86	86.65	1.83
<i>TMFAug</i> (\mathcal{P}^2) (w/o filtering)	71.72	74.09	77.74	78.26	84.06	82.47	84.30	<u>86.92</u>	<u>86.55</u>	86.38	84.55	86.85	2.67
<i>TMFAug</i> (\mathcal{P}^2)	73.83	75.93	78.28	79.33	84.82	84.57	85.36	86.41	86.39	87.12	86.38	86.86	1.42
<i>TMFAug</i> ($\mathcal{P}^1 + \mathcal{P}^2$) (w/o refinement)	72.51	75.66	78.29	77.23	85.09	84.57	85.63	86.66	85.60	87.74	85.07	86.96	1.75
<i>TMFAug</i> ($\mathcal{P}^1 + \mathcal{P}^2$) (w/o filtering)	67.27	71.22	57.09	66.76	84.05	<u>83.52</u>	85.87	<u>86.92</u>	85.91	84.61	<u>87.44</u>	83.13	2.42
<i>TMFAug</i> ($\mathcal{P}^1 + \mathcal{P}^2$)	<u>72.25</u>	76.96	<u>76.98</u>	<u>77.23</u>	85.09	83.26	86.15	86.66	85.92	<u>87.68</u>	85.08	<u>86.59</u>	1.67

make the following reasonable explanation. Both random-walk-based methods and GNN-based methods can learn structured account features during detection, while our module can also capture structured behavior features, these two parts can be organically combined and bring consistent positive gains. These phenomena provide a positive answer to **RQ1**, indicating that the *TMFAug* module can benefit the existing Ponzi detection methods via feature augmentation and improve their performance without adjusting them.

D. Superiority of Temporal Information (**RQ2**)

After evaluating the overall performance of our method, we further investigate the superiority of time-aware metapaths over time-less ones. By comparing the two modules (*TMFAug* and *MFAug*) in Table IV, we observe that methods with *TMFAug* outperform those with *MFAug* at most cases. Specifically, *TMFAug* achieves a higher average performance ranking than *MFAug*, i.e., $Rank(3.50) > Rank(3.83)$ in \mathcal{P}^1 , $Rank(2.75) > Rank(3.33)$ in \mathcal{P}^2 , $Rank(3.17) > Rank(3.42)$ in $(\mathcal{P}^1 + \mathcal{P}^2)$. These phenomena provide a positive answer to **RQ2**, indicating that the temporal behavior patterns captured by the *TMFAug* module are more effective for improving Ponzi detection than timeless ones.

E. Impact of Behavior Pattern (**RQ3**)

We further investigate the impact of different behavior patterns on detecting Ponzi schemes. Specifically, we compare a total of six combinations of different metapaths (\mathcal{P}^1 , \mathcal{P}^2 and $\mathcal{P}^1 + \mathcal{P}^2$) and different modules (*TMFAug* and *MFAug*), as shown in Table IV. As we can see, for *TMFAug* or *MFAug*, the performance ranking of different metapaths is consistent: $TMFAug(\mathcal{P}^2) > TMFAug(\mathcal{P}^1 + \mathcal{P}^2) > TMFAug(\mathcal{P}^1)$ and $MFAug(\mathcal{P}^2) > MFAug(\mathcal{P}^1 + \mathcal{P}^2) > MFAug(\mathcal{P}^1)$, which suggests that the enhancement effect relies on the choice of metapaths and answers to **RQ3**. Both \mathcal{P}^1 and \mathcal{P}^2 are extracted from the basic behavior patterns of Ponzi and normal accounts defined in Eq. (4), and we have reasonable explanations for their performance difference. As shown in Table III, the number of \mathcal{P}^1 far exceeds that of \mathcal{P}^2 , even with the existence of relation merging and behavior filtering, the number of

retained super metapaths is still huge, which inevitably leads to information redundancy and over-smoothing during feature aggregation. On the other hand, compared with \mathcal{P}^1 , \mathcal{P}^2 contains more diverse and fine-grained behavior patterns, which can better characterize the differences between Ponzi accounts and normal accounts. In addition, this is also illustrated by the results on manual feature engineering and Line, e.g., aggregating features from \mathcal{P}^1 may lead to a negative gain in performance.

F. Impact of Behavior Refinement (**RQ4**)

Behavior refinement is proposed to characterize different behavior patterns in fine granularity, and we further investigate its effectiveness. Table V reports the performance comparison of *TMFAug* with and without behavior refinement. Overall, we can observe that *TMFAug* with behavior refinement achieves a higher average local ranking across different metapaths, i.e., $Rank(1.67) = Rank(1.67)$ in \mathcal{P}^1 , $Rank(1.42) > Rank(1.83)$ in \mathcal{P}^2 , and $Rank(1.67) > Rank(1.75)$ in $(\mathcal{P}^1 + \mathcal{P}^2)$. Furthermore, behavior refinement works better on \mathcal{P}^2 , manifested as a larger ranking boost. Here we combine the properties of different metapaths to provide further analysis. First, \mathcal{P}^1 has a straightforward structure, so we can just refine it into two cases. Despite the behavior refinement, simple interactions do not lead to more discriminative patterns, nor do they further yield gains. While \mathcal{P}^2 has a more complex structure and contains more behavior patterns, especially patterns unique to normal accounts, and thus can be refined into four cases. Behavior refinement can process coarse-grained information into fine-grained and discriminative patterns, so it is more beneficial for more complex \mathcal{P}^2 . Moreover, behavior refinement can help to better perform subsequent behavior filtering. These phenomena provide a positive answer to **RQ4**, indicating that the *TMFAug* somewhat relies on behavior refinement, and the more complex interaction patterns access to their superior performance.

G. Impact of Behavior Filtering (**RQ5**)

Behavior filtering is proposed to alleviate information redundancy and feature explosion during metapath feature ag-

gregation, and we further investigate its effectiveness. Table V reports the performance comparison of *TMFAug* with and without behavior filtering. Overall, we can observe that *TMFAug* with behavior filtering achieves a higher average local ranking across different metapaths, i.e., $Rank(1.67) > Rank(2.50)$ in \mathcal{P}^1 , $Rank(1.42) > Rank(2.67)$ in \mathcal{P}^2 , and $Rank(1.67) > Rank(2.42)$ in $(\mathcal{P}^1 + \mathcal{P}^2)$, indicating its effectiveness. In this regard, we make the following reasonable explanation. Without behavior filtering, metapaths are not only redundant in number, but also contain much unimportant information. When updating node features along metapaths, using too many metapaths could make the information jumbled, and those unimportant metapaths will interfere with the subsequent detection. In addition, behavior filtering is more beneficial for manual feature engineering and Line, in which the highest relative improvement rate reaches 34.84%. We speculate that integrating excessive metapaths will greatly destroy the original feature representation of manual feature engineering and Line due to the weak robustness of their initial features. And for DeepWalk, Node2Vec and GNN-based methods, behavior filtering also yields some gains, but only marginally. The reason for the low gain is that the learned embeddings are robust and have richer structural and semantic information than the manual feature engineering and Line, so noisy metapaths do not severely affect them. These phenomena provide a positive answer to **RQ5**, indicating that the behavior filtering can effectively alleviate information redundancy and feature explosion during metapath feature aggregation, further improving Ponzi detection.

VI. CONCLUSION

Existing methods for Ponzi scheme detection usually neglect complex and temporal interaction behaviors. In this paper, we propose a Time-aware Metapath Feature Augmentation module, which includes symbiotic relationship merging, behavior refinement and filtering, and metapath feature aggregation. This module can effectively capture the real metapath-based transaction patterns and aggregate the temporal behavior information during Ponzi scheme detection on Ethereum. Experiments show that this module can significantly improve the performance of exciting Ponzi scheme detection methods. Light of the fact that the current method requires expert knowledge to capture metapaths, which is time-consuming. Our future research will attempt to reduce the manual definition of metapaths, for instance by automatically learning metapaths [36]–[38] to save time and improve generalization.

REFERENCES

- [1] X. Li, P. Jiang, T. Chen, X. Luo, and Q. Wen, "A survey on the security of blockchain systems," *Future Generation Computer Systems*, vol. 107, pp. 841–853, 2020.
- [2] D. R. Stinson, *Cryptography: theory and practice*. Chapman and Hall/CRC, 2005.
- [3] B. Lashkari and P. Musilek, "A comprehensive review of blockchain consensus mechanisms," *IEEE Access*, vol. 9, pp. 43 620–43 652, 2021.
- [4] S. Nakamoto, "Bitcoin: A peer-to-peer electronic cash system," *Decentralized Business Review*, p. 21260, 2008.
- [5] V. Buterin *et al.*, "A next-generation smart contract and decentralized application platform," *white paper*, vol. 3, no. 37, pp. 2–1, 2014.
- [6] G. Wood *et al.*, "Ethereum: A secure decentralised generalised transaction ledger," *Ethereum project yellow paper*, vol. 151, no. 2014, pp. 1–32, 2014.
- [7] S. Wang, L. Ouyang, Y. Yuan, X. Ni, X. Han, and F.-Y. Wang, "Blockchain-enabled smart contracts: architecture, applications, and future trends," *IEEE Transactions on Systems, Man, and Cybernetics: Systems*, vol. 49, no. 11, pp. 2266–2277, 2019.
- [8] M. Artzrouni, "The mathematics of ponzi schemes," *Mathematical Social Sciences*, vol. 58, no. 2, pp. 190–201, 2009.
- [9] T. Kell, H. Yousaf, S. Allen, S. Meiklejohn, and A. Juels, "Forage: Anatomy of a smart-contract pyramid scheme," *arXiv preprint arXiv:2105.04380*, 2021.
- [10] D. Macpherson, "A survey of homogeneous structures," *Discrete Mathematics*, vol. 311, no. 15, pp. 1599–1634, 2011.
- [11] J. Zhou, C. Hu, J. Chi, J. Wu, M. Shen, and Q. Xuan, "Behavior-aware account de-anonymization on ethereum interaction graph," *IEEE Transactions on Information Forensics and Security*, vol. 17, pp. 3433–3448, 2022.
- [12] C. Shi, Y. Li, J. Zhang, Y. Sun, and S. Y. Philip, "A survey of heterogeneous information network analysis," *IEEE Transactions on Knowledge and Data Engineering*, vol. 29, no. 1, pp. 17–37, 2016.
- [13] Y. Sun, J. Han, X. Yan, P. S. Yu, and T. Wu, "Pathsim: Meta path-based top-k similarity search in heterogeneous information networks," *Proceedings of the VLDB Endowment*, vol. 4, no. 11, pp. 992–1003, 2011.
- [14] Y. Dong, N. V. Chawla, and A. Swami, "Metapath2vec: Scalable Representation Learning for Heterogeneous Networks," in *Proceedings of the 23rd ACM SIGKDD international conference on knowledge discovery and data mining*, 2017, pp. 135–144.
- [15] C. Shi, B. Hu, W. X. Zhao, and S. Y. Philip, "Heterogeneous information network embedding for recommendation," *IEEE Transactions on Knowledge and Data Engineering*, vol. 31, no. 2, pp. 357–370, 2018.
- [16] B. Perozzi, R. Al-Rfou, and S. Skiena, "Deepwalk: Online learning of social representations," in *Proceedings of the 20th ACM SIGKDD international conference on Knowledge discovery and data mining*, 2014, pp. 701–710.
- [17] A. Grover and J. Leskovec, "node2vec: Scalable feature learning for networks," in *Proceedings of the 22nd ACM SIGKDD international conference on Knowledge discovery and data mining*, 2016, pp. 855–864.
- [18] J. Tang, M. Qu, M. Wang, M. Zhang, J. Yan, and Q. Mei, "Line: Large-scale information network embedding," in *Proceedings of the 24th international conference on world wide web*, 2015, pp. 1067–1077.
- [19] T. N. Kipf and M. Welling, "Semi-supervised classification with graph convolutional networks," *arXiv preprint arXiv:1609.02907*, 2016.
- [20] P. Velickovic, G. Cucurull, A. Casanova, A. Romero, P. Lio, and Y. Bengio, "Graph attention networks," *stat*, vol. 1050, p. 20, 2017.
- [21] W. Hamilton, Z. Ying, and J. Leskovec, "Inductive representation learning on large graphs," *Advances in neural information processing systems*, vol. 30, 2017.
- [22] K. Xu, W. Hu, J. Leskovec, and S. Jegelka, "How powerful are graph neural networks?" *arXiv preprint arXiv:1810.00826*, 2018.
- [23] T. Moore, J. Han, and R. Clayton, "The postmodern ponzi scheme: Empirical analysis of high-yield investment programs," in *International Conference on financial cryptography and data security*. Springer, 2012, pp. 41–56.
- [24] M. Vasek and T. Moore, "There's no free lunch, even using bitcoin: Tracking the popularity and profits of virtual currency scams," in *International conference on financial cryptography and data security*. Springer, 2015, pp. 44–61.
- [25] W. Chen, Z. Zheng, J. Cui, E. Ngai, P. Zheng, and Y. Zhou, "Detecting ponzi schemes on ethereum: Towards healthier blockchain technology," in *Proceedings of the 2018 world wide web conference*, 2018, pp. 1409–1418.
- [26] Y. Chen, H. Dai, X. Yu, W. Hu, Z. Xie, and C. Tan, "Improving ponzi scheme contract detection using multi-channel textcnn and transformer," *Sensors*, vol. 21, no. 19, p. 6417, 2021.
- [27] S. Fan, S. Fu, H. Xu, and C. Zhu, "Expose your mask: smart ponzi schemes detection on blockchain," in *2020 International Joint Conference on Neural Networks (IJCNN)*. IEEE, 2020, pp. 1–7.
- [28] Y. Zhang, W. Yu, Z. Li, S. Raza, and H. Cao, "Detecting ethereum ponzi schemes based on improved lightgbm algorithm," *IEEE Transactions on Computational Social Systems*, 2021.
- [29] S. Yu, J. Jin, Y. Xie, J. Shen, and Q. Xuan, "Ponzi scheme detection in ethereum transaction network," in *International Conference on Blockchain and Trustworthy Systems*. Springer, 2021, pp. 175–186.

[30] H. Zhang, J. Yu, B. Yan, M. Jing, and J. Zhao, "Security on ethereum: Ponzi scheme detection in smart contract," in *International Conference on Algorithmic Applications in Management*. Springer, 2022, pp. 435–443.

[31] M. Bartoletti, S. Carta, T. Cimoli, and R. Saia, "Dissecting ponzi schemes on ethereum: identification, analysis, and impact," *Future Generation Computer Systems*, vol. 102, pp. 259–277, 2020.

[32] J. Jin, J. Zhou, C. Jin, S. Yu, Z. Zheng, and Q. Xuan, "Dual-channel early warning framework for ethereum ponzi schemes," *The 7th China National Conference on Big Data and Social Computing*, 2022.

[33] C. Jin, J. Jin, J. Zhou, J. Wu, and Q. Xuan, "Heterogeneous feature augmentation for ponzi detection in ethereum," *IEEE Transactions on Circuits and Systems II: Express Briefs*, 2022.

[34] W. S. Noble, "What is a support vector machine?" *Nature biotechnology*, vol. 24, no. 12, pp. 1565–1567, 2006.

[35] M. R. Segal, "Machine learning benchmarks and random forest regression," 2004.

[36] L. Wang, C. Gao, C. Huang, R. Liu, W. Ma, and S. Vosoughi, "Embedding heterogeneous networks into hyperbolic space without meta-path," in *Proceedings of the AAAI conference on artificial intelligence*, vol. 35, no. 11, 2021, pp. 10 147–10 155.

[37] Y. Chang, C. Chen, W. Hu, Z. Zheng, X. Zhou, and S. Chen, "Megnn: Meta-path extracted graph neural network for heterogeneous graph representation learning," *Knowledge-Based Systems*, vol. 235, p. 107611, 2022.

[38] S. Yun, M. Jeong, R. Kim, J. Kang, and H. J. Kim, "Graph transformer networks," *Advances in neural information processing systems*, vol. 32, 2019.



Qi Xuan (M'18) received the BS and PhD degrees in control theory and engineering from Zhejiang University, Hangzhou, China, in 2003 and 2008, respectively. He was a Post-Doctoral Researcher with the Department of Information Science and Electronic Engineering, Zhejiang University, from 2008 to 2010, respectively, and a Research Assistant with the Department of Electronic Engineering, City University of Hong Kong, Hong Kong, in 2010 and 2017. From 2012 to 2014, he was a Post-Doctoral Fellow with the Department of Computer Science, University of California at Davis, CA, USA. He is a senior member of the IEEE and is currently a Professor with the Institute of Cyberspace Security, College of Information Engineering, Zhejiang University of Technology, Hangzhou, China. His current research interests include network science, graph data mining, cyberspace security, machine learning, and computer vision.



Chengxiang Jin received the BS degree in electrical engineering and automation from Zhejiang University of Science and Technology, Hangzhou, China, in 2021. He is currently pursuing the MS degree in control theory and engineering at Zhejiang University of Technology, Hangzhou, China. His current research interests include graph data mining and blockchain data analytics, especially for heterogeneous graph mining in Ethereum.



Jiajun Zhou received the BS degree in automation from the Zhejiang University of Technology, Hangzhou, China, in 2018, where he is currently pursuing the Ph.D degree in control theory and engineering with the College of Information and Engineering. His current research interests include graph data mining and deep learning, especially for graph self-supervised learning and blockchain data analytics.



Jie Jin received the BS degree in automation from Hunan International Economics University, Hunan, China, in 2020. He is currently pursuing the MS degree at the College of Information Engineering, Zhejiang University of Technology, Hangzhou, China. His current research interests include Graph data mining and Blockchain Data Analyse.



Jiajing Wu (Senior Member, IEEE) received the Ph.D. degree from The Hong Kong Polytechnic University, Hong Kong, in 2014. In 2015, she joined Sun Yat-sen University, Guangzhou, China, where she is currently an Associate Professor. Her research interests include blockchain, graph mining, and network science. Dr. Wu was awarded the Hong Kong Ph.D. Fellowship Scheme during her Ph.D. degree in Hong Kong from 2010 to 2014. She also serves as an Associate Editor for IEEE TRANSACTIONS ON CIRCUITS AND SYSTEMS II: EXPRESS